Chapter 5

Vibration Control of Flexible Structures Using Semi-Active Mount : Experimental Investigation

Seung-Bok Choi, Sung Hoon Ha and Juncheol Jeon

Additional information is available at the end of the chapter

http://dx.doi.org/10.5772/48823

1. Introduction

In many dynamic systems such as robot and aerospace areas, flexible structures have been extremely employed to satisfy various requirements for large scale, light weight and high speed in dynamic motion. However, these flexible structures are readily susceptible to the internal/external disturbances (or excitations). Therefore, vibration control schemes should be exerted to achieve high performance and stability of flexible structure systems. Recently, in order to successfully achieve vibration control for flexible structures smart materials such as piezoelectric materials [1-2], shape memory alloys [3-4], electrorheological (ER) fluids [5-6] and magnetorheological (MR) fluids [7] are being widely utilized. Among these smart materials, ER or MR fluid exhibits reversible changes in material characteristics when subjected to electric or magnetic field. The vibration control of flexible structures using the smart ER or MR fluid can be achieved from two different methods. The first approach is to replace conventional viscoelastic materials by the ER or MR fluid. This method is very effective for shape control of flexible structures such as plate [5]. The second approach is to devise dampers or mounts and apply to vibration control of the flexible structures. This method is very useful to isolate vibration of large structural systems subjected to external excitations [6-7]. In this work, a new type of MR mount is proposed and applied to vibration control of the flexible structures.

In order to reduce unwanted vibration of the flexible structure system, three different types of mounts are normally employed: passive, semi-active and active. The passive rubber mount, which has low damping, shows efficient vibration performance at the non-resonant and high frequency excitation. Thus, the rubber mount is the most popular method applied for various vibrating systems. However, it cannot have a favorable performance due to small damping effect at the resonant frequency excitation. On the other hand, the passive hydraulic mount has been developed to utilize dynamic absorber effect or meet large damping requirement in the resonance of low frequency domain [8]. However, the high dynamic stiffness property of the hydraulic mount may deteriorate isolation performance in the non-resonant excitation domain. Thus, the damping and stiffness of the passive mounts are not simultaneously controllable to meet imposed performance criteria in a wide frequency range. The active mounts are normally operated by using external energy supplied by actuators in order to generate control forces on the system subjected to excitations [9]. The control performance of the active mount is fairly good in a wide frequency range, but its cost is expensive. Moreover, its configuration is complex and its stability may not be guaranteed in a certain operation condition. On the other hand, the semi-active mounts cannot inject mechanical energy into the structural systems. But, it can adjust damping to reduce unwanted vibration of the flexible structure systems. It is known that using the controllable yield stress of ER or MR fluid, a very effective semi-active mount can be devised for vibration control of the flexible structures. The flow operation of the ER or MR mount can be classified into three different modes: shear mode [6], flow mode [10] and squeeze mode [11].

In this article, a new type of semi-active MR mount shown in the figure 1 is proposed and applied to vibration control of flexible structures. As a first step to achieve the research goal, the configuration of a mixed-mode MR mount is devised and the mathematical model is formulated on the basis of non-dimensional Bingham number. After manufacturing an appropriate size of MR mount, the field-dependent damping force is experimentally evaluated with respect to the field intensity. The MR mount is installed on the beam structure as a semi-active actuator, while the beam structure is supported by two passive rubber mounts. The dynamic model of the structural system incorporated with the MR mount is then derived in the modal coordinate, and an optimal controller is designed in order to control unwanted vibration responses of the structural system subjected to external excitations. The controller is experimentally implemented and control performances such as acceleration of the structural systems are evaluated in frequency domain.

2. MR Mount

In this work, a new type of the mixed-mode MR mount which is operated under the flow and shear motion is proposed. The schematic configuration of the MR mount proposed in this work is shown in Figure 1 (a). The MR mount consists of rubber element and MR dash-pot. The MR dash-pot is assembled by MR fluid, piston (or plunger), electromagnet coil, flux guide, and housing. The MR fluid is filled in the gap between piston and outer cylindrical housing. The electromagnetic coil is wired inside of the cylindrical housing. The housing can be fixed to the supporting structure, and the plunger is attached to the top end of the rubber element. The rubber element has a role to support the static load and isolate the vibration transmission at the non-resonant and high frequency regions. During the relative motion of the plunger and housing, MR fluid flows through annular gap. Thus, the pressure drop due

http://dx.doi.org/10.5772/48823

to flow resistance of MR fluid in the annular gap can be obtainable. At the same time, the MR dash-pot has additional shear resistance due to relative motion of annular gap walls. Therefore, the proposed MR dash-pot operates under both the flow and shear modes. If no magnetic field is applied, the MR dash-pot only produces a damping force caused by the fluid resistance associated with the viscosity of the MR fluid. However, if the magnetic field is applied through the annular gap, the MR mount produces a controllable damping force due to the yield stress of the MR fluid. As it can be seen from Figure 1 (a), the proposed MR mount has compact structure and operates without frictional components.

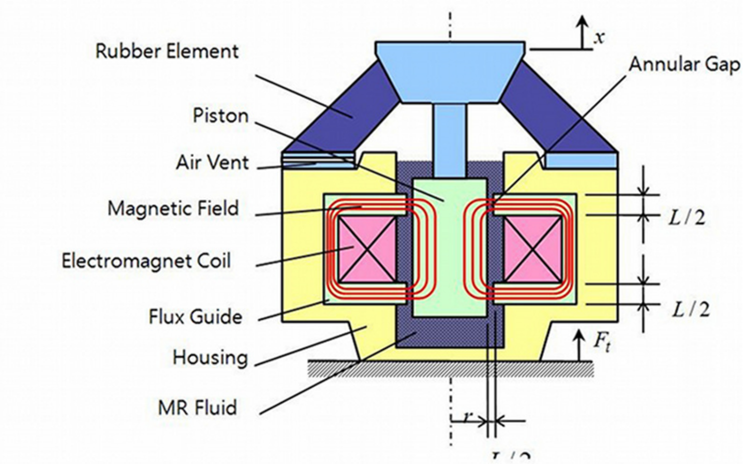

(a) configuration

(b) photograph

Figure 1. The proposed MR mount.

The transmitted force (F_t) through the proposed MR mount can be represented by

$$F_t = k_r x + c_r \dot{x} + F_{mr} \tag{1}$$

In the above, k_r and c_r are stiffness and damping of the rubber element, respectively. x is the deflection of the rubber element. The damping force (F_{mr}) due to the flow resistance of the MR fluid in the gap can be represented by considering the plug flow of the MR fluid under the mixed mode operation as follows [7].

$$\varphi_F = a\varphi_r^{\,3} + \left(\frac{b}{6}\varphi_c + c\right)\varphi_r^{\,2} \tag{2}$$

where,

$$\varphi_F = \frac{F_{mr}}{6\pi\eta v_p L},\ \varphi_c = \frac{\tau_y h}{\eta v_p},\ \varphi_r = \frac{r}{h} \tag{3}$$

In the above, φ_F is the dimensionless damping force, φ_c is the Bingham number, and φ_r is the dimensionless geometric parameter. η is the post-yield plastic viscosity, v_p is the relative velocity between piston and housing, L is the annular gap length, τ_y is the field-dependent yield shear stress of the MR fluid, h is the annular gap size, and r is the piston radius. The dimensionless parameter φ_c represents the ratio of the dynamic yield shear stress to the viscous shear stress. Moreover, φ_c shows the influence of the magnetic field on the damping force of the MR mount. The dimensionless geometric parameter φ_r is characterized by the piston radius r and gap size h . The dimensionless damping force φ_F increases as the Bingham number φ_c and dimensionless geometric parameter φ_r increase. This implies that high yield stress and large piston area are required to generate high damping force of the MR mount. On the other hand, the gap length L depends on the dimensionless damping force φ_F only. Therefore, the damping force F_{mr} can be directly scaled by the gap length L . It is noted that the damping force F_{mr} can be expressed by the velocity of rubber element and the field-dependent yield shear stress of the MR fluid. The parameters a and c of equation (2) are chosen to be 1 by considering Newtonian flow behavior of the MR fluid in the absence of magnetic field. And then, the parameter b , which reflects the effect of Bingham flow of the MR fluid, is chosen to be 2.47 using a least square error criterion.

The field-dependent yield stress τ_y of the MR fluid (MRF-132LD, Lord Corporation) employed in this study has been experimentally obtained by $0.13H^{1.3}$ kPa. Here the unit of magnetic field H is kA/m. The post-yield plastic viscosity η was also experimentally evaluated by 0.59 Pasec. The rheometer (MCR300, Physica, Germany) was used for obtaining the value of the yield stress and the post-yield plastic viscosity. By considering both the nondimensional damping force equations (2,3) and the size of the structural system, an appropriate size of MR mount was designed and manufactured as shown in Figure 1 (b). The piston radius r , gap size h , and gap length L are designed to be 8.5 mm, 1.5 mm, and 10 mm, respectively. The field-dependent damping force is predicted and experimentally measured by exciting the MR mount with the sinusoidal signal which has frequency of 15 Hz and amplitude of 0.07m/sec. Figure 2 presents controllable damping force characteristic of the proposed MR mount. In order to measure the field-dependent damping force of the MR mount, the MR mount is placed between the load cell and electromagnetic exciter. When the shaker table moves up and down by a command signal generated from the exciter controller, the MR mount produces the damping force and it is measured by the load cell. As expected, as the input current increases, the damping force also increases. It is also observed that the predicted field-dependent damping force shows small difference from the measured force in the post-yield velocity region. On the other hand, the damping forces show much large difference in the pre-yield region. This is because the model (2,3) is discontinuous and cannot represent the hysteretic behavior of the MR mount in the transition from pre-yield to post-yield.

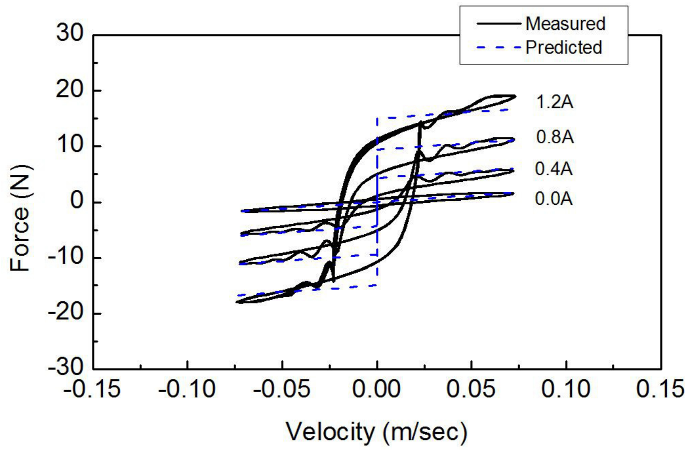

Figure 2. The field-dependent damping force of the MR mount.

The nondimensional form (2,3) of MR mount under mixed mode can be transformed to the Bingham plastic model as follows [12]. This simple model is widely used for the controller implementations.

$$F_{mr} = c_f(I)v_p + F_y(I)\mathrm{sgn}(v_p) \tag{4}$$

In the above, c_f and F_y are the post-yield damping constant and the yield force, respectively. I is the current applied to the MR mount. In order to identify the parameters of the models, a constrained least-mean-squared (LMS) error minimization procedure is used. The cost function J for Bingham plastic model is defined by

$$J(c_f, F_y) = \sum_{k=1}^{N}\left[f(t_k) - \hat{f}(t_k)\right]^2 \tag{5}$$

where $\hat{f}(t_k)$ is the force calculated using the model given by equation (4), $f(t_k)$ is the measured force shown in figure 2, and t_k is the time at which the kth sample has been taken. Parameters c_f and F_y of the Bingham plastic model are estimated so as to minimize the cost function J . The parameter optimization is performed on a test case of the identification data set. It is noted that the optimization procedure is applied to the data of the post-yield regions for Bingham plastic model. Based on the measured response in Figure 2, the field-dependent damping constant c_f and yield force F_y are identified by $(23 + 25I)$ Nsec/m and

$8.28I^{1.85}$ N, respectively. Here, the unit of current I is A. These values will be used as system parameters in the controller implementation for the structural system.

3. Structural System

In order to investigate the applicability of the proposed MR mount to vibration control, a flexible structure system is established as shown in Figure 3. The MR mount is placed between the exciting mass and steel beam structure. When the mass is excited by external disturbance, the force transmitting through the MR mount excites the beam structure. Thus, the vibration of the beam structure can be controlled by activating the MR mount. $y(p_j)$ is the displacement at position p_j of the structural system. The MR mount is placed at position p_2 of the beam structure, while two passive rubber mounts are placed at p_1 and p_3 to support the beam structure. The governing equation of the motion of the proposed structural system can be obtained using the mode summation method as follows [13]:

$$\ddot{q}_i(t) + 2\zeta_i\omega_i\dot{q}_i(t) + \omega_i^2 q_i(t) = \frac{Q_i(t)}{I_i} + \frac{Q_{exi}(t)}{I_i},\ i = 1,\ 2,\ \cdots,\ \infty \tag{6}$$

where,

$$Q_i(t) = (\varphi_i(p_4) - \varphi_i(p_2))(-F_{mr}(t)) \tag{7}$$

$$Q_{ex_i}(t) = \varphi_i(p_4)F_{ex}(t) \tag{8}$$

In the above, $q_i(t)$ is the generalized modal coordinate, $\varphi_i(x)$ is the mode shape value at position x , ω_i is the modal frequency, ζ_i is the damping ratio, and I_i is the generalized mass of the i th mode. $Q_i(t)$ is the generalized force including the damping force of the MR mount, and $Q_{exi}(t)$ is the generalized force including the exciting force $F_{ex}(t)$. It is noted that the spring and damping effects of the rubber elements are resolved in the modal parameters of the structural system.

In order to determine system parameters such as modal frequencies and mode shapes, modal analysis is undertaken by adopting a commercial software (MSC/NASTRAN for Windows V4.0). The finite element model of the flexible structure consists of 30 beam elements, 3 spring elements, and 2 mass elements. The nodes of the structural system are constrained in the x, z directions, and the 2-node elastic beam element is used to model the beam. The geometry of the steel beam is 1500mm (length) 60mm (length) 15mm (thickness). The rubber mounts are placed on the 50mm (p_1) and 1450mm (p_3) from left end of the beam. The MR mount is placed on the 600mm (p_2) from the left end of the beam instead of the center of the beam. This is because that the MR mount located at center of the beam cannot control the rotational modes. The 2-node spring elements are used to model the rubber mounts and rubber element of the MR mount. The material property for the spring elements is set by 60kN/m which has been experimentally evaluated. To model the mass of lower part of the MR mount and vibrating mass, the 1-node lumped mass element is used. The material properties for the mass elements are 1.5kg and 3kg for the lower part of the MR mount and the vibrating mass, respectively.

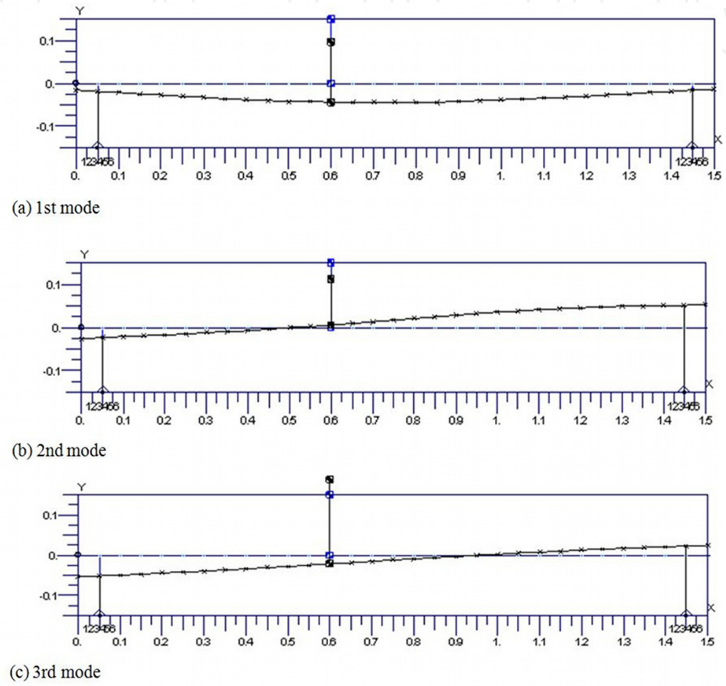

Figure 3. Configuration of the structural system with the MR mount.

Figure 4 presents mode shapes of the first three modes. The first mode is bending mode, while the second and the third modes are combination of rotational and bending modes. In this study, modal parameters of the structural system are identified by experimental modal test. It is evaluated by computer simulation that the effect of the residual modes is quite small compared with dominant mode. Therefore, in this paper, only dominant modes are considered.

Figure 5 shows the schematic configuration of the experimental setup for the modal parameter identification. The mass on the MR mount is excited by the electromagnetic exciter. The MR mount is removed for the modal parameter identification of structure system only. Thus, this test shows the modal test of the passive structural system in which the mass is supported by the rubber mount. The excitation force and frequency are regulated by the exciter controller. Accelerometers are attached to the mass and beam, and their positions are denoted by $x = p_1$, $x = p_2$, $x = p_3$ and $x = p_4$. From this, the following system parameters are obtained : ω_1 56.9 rad/s, ω_2 144.8 rad/s, ω_3 168.4 rad/s, ζ_1 0.0260, ζ_2 0.0497, and ζ_3 0.0630.

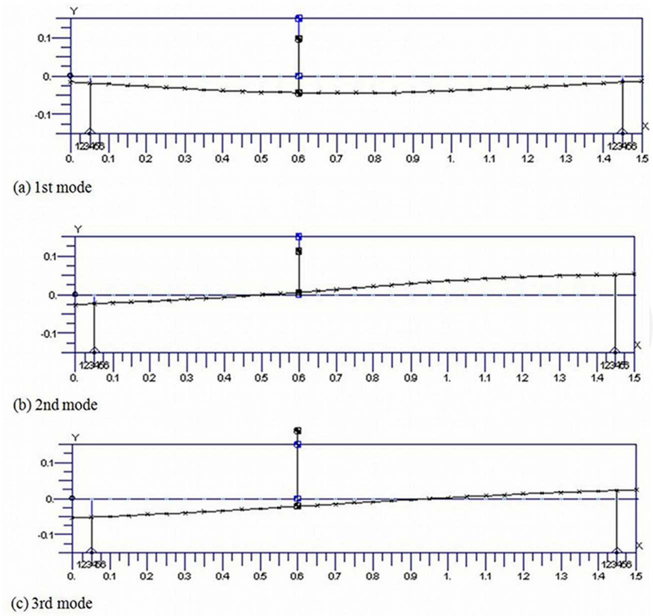

Figure 4. Mode shapes of the structural system.

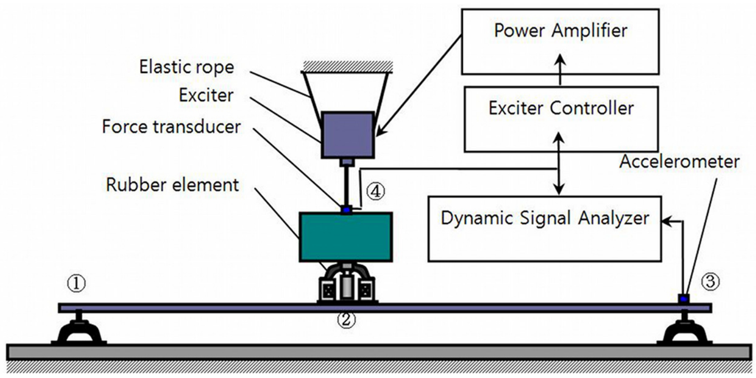

Figure 5. Experimental setup for the modal test of MR fluid mount system.

By considering first three modes as controllable modes, the dynamic model of the structural system, given by equations (6-8), can be expressed in a state space control model as follows.

$$\dot{x}(t) = Ax(t) + Bu(t) + \boldsymbol{w}_1 \tag{9}$$

$$y(t) = \boldsymbol{C}x(t) + \boldsymbol{w}_2 \tag{10}$$

where

$$\boldsymbol{x}(t) = [q_1(t)\dot{q}_1(t)q_2(t)\dot{q}_2(t)q_3(t)\dot{q}_3(t)]^T \tag{11}$$

$$\boldsymbol{y}(t)=[\dot{y}(p_4, t)\dot{y}(p_2, t)]^T \tag{12}$$

$$u(t)=[F_{mr}(t)] \tag{13}$$

$$A=\begin{bmatrix} 0 & 1 & 0 & 0 & 0 & 0 \\ -\omega_1^2 & -2\zeta_1\omega_1 & 0 & 0 & 0 & 0 \\ 0 & 0 & 0 & 1 & 0 & 0 \\ 0 & 0 & -\omega_2^2 & -2\zeta_2\omega_2 & 0 & 0 \\ 0 & 0 & 0 & 0 & 0 & 1 \\ 0 & 0 & 0 & 0 & -\omega_3^2 & -2\zeta_3\omega_3 \end{bmatrix} \tag{14}$$

$$\boldsymbol{B}=\begin{bmatrix} 0 \\ (\varphi_1(p_2)-\varphi_1(p_4))/I_1 \\ 0 \\ (\varphi_2(p_2)-\varphi_2(p_4))/I_2 \\ 0 \\ (\varphi_3(p_2)-\varphi_3(p_4))/I_3 \end{bmatrix} \tag{15}$$

$$\boldsymbol{C}=\begin{bmatrix} 0 & \varphi_1(p_4) & 0 & \varphi_2(p_4) & 0 & \varphi_3(p_4) \\ 0 & \varphi_1(p_2) & 0 & \varphi_2(p_2) & 0 & \varphi_3(p_2) \end{bmatrix} \tag{16}$$

In the above, $x(t)$ is the state vector, $\boldsymbol{y}(t)$ is the measured output vector, A is the system matrix, B is the control input matrix, $\boldsymbol{C}$ is the output matrix, and $u(t)$ is the control input. $\boldsymbol{w}_1$ and $\boldsymbol{w}_2$ are uncorrelated white noise characterized by covariance matrices $\boldsymbol{V}_1$ and $\boldsymbol{V}_2$ as follows [14].

$$\begin{aligned} Cov(\boldsymbol{w}_1, \boldsymbol{w}_1^T)&=\boldsymbol{V}_1 \\ Cov(\boldsymbol{w}_2, \boldsymbol{w}_2^T)&=\boldsymbol{V}_2 \\ Cov(\boldsymbol{w}_1, \boldsymbol{w}_2^T)&=0 \end{aligned} \tag{17}$$

4. Vibration Control

In order to attenuate unwanted vibration of the flexible structural system, the linear quadratic Gaussian (LQG) controller, consisting of linear quadratic regulator (LQR) and Kalman-Bucy filter (KBF), is adopted. As a first step to formulate the LQG controller the performance index (J) to be minimized is given by

$$J = \int_0^{\infty} \{ \boldsymbol{x}^T(t)\boldsymbol{Q}\boldsymbol{x}(t) + u^T(t)Ru(t) \} dt \tag{18}$$

In the above, $\boldsymbol{Q}$ is the state weighting semi-positive matirx and R is the input weighting positive constant. Since the system (A, B) in equation (9) is controllable, the LQR controller for the MR mount can be obtained as follows.

$$u(t) = -\boldsymbol{P}^{-1}\boldsymbol{B}^T\boldsymbol{x}(t) = -\boldsymbol{K}\boldsymbol{x}(t) \tag{19}$$

In the above, $\boldsymbol{K}$ is the state feedback gain matrix, and $\boldsymbol{P}$ is the solution of the following algebraic Riccati equation :

$$A^T P + PA - PBR^{-1}B^T P + Q = 0 \tag{20}$$

Thus, the control force of the MR mount can be represented as

$$\begin{aligned} u(t) &= -\boldsymbol{K}\boldsymbol{x}(t) \\ &= -(k_1 q_1(t) + k_2 \dot{q}_1(t) + k_3 q_2(t) + k_4 \dot{q}_2(t) + k_5 q_3(t) + k_6 \dot{q}_3(t)) \end{aligned} \tag{21}$$

In this work, by the tuning method the control gains of the k_1 , k_2 , k_3 , k_4 , k_5 and k_6 are selected by -536068, 8315.9, -327595, 3706.3, -15.99 and 2359.4, respectively. On the other hand, the proposed MR mount is semi-active. Therefore, the control signal needs to be applied according to the following actuating condition [15]:

$$u(t) = \begin{bmatrix} u(t), & for\, u(t)(\dot{y}(p_4, t) - \dot{y}(p_2, t))0 \\ 0 \;\; , & for\, u(t)(\dot{y}(p_4, t) - \dot{y}(p_2, t)) \le 0 \end{bmatrix} \tag{22}$$

This condition physically indicates that the actuating of the controller $u(t)$ assures the increment of energy dissipation of the stable system.

Since the states of $q_i(t)$ and $\dot{q}_i(t)$ of the LQR controller (21) are not available from direct measurement, the Kalman-Bucy filter (KBF) is formulated. The KBF is a state estimator which is optimally considered in the statistical sense. The estimated state, $\hat{\boldsymbol{x}}(t)$, can be obtained from the following state observer [14].

$$\hat{x}(t) = A\hat{x}(t) + Bu(t) + \boldsymbol{L}\ (\boldsymbol{y}(t) - \boldsymbol{C}\hat{x}(t)) \tag{23}$$

where,

$$\boldsymbol{L} = \boldsymbol{O}\boldsymbol{C}^T\boldsymbol{V}_2^{-1} = \begin{bmatrix} l_{11} l_{12} \cdots l_{16} \\ l_{21} l_{22} \cdots l_{26} \end{bmatrix}^T \tag{24}$$

http://dx.doi.org/10.5772/48823

In the above, L is the observer gain matrix, and O is the solution of the following observer

Riccati equation :

$$AO + OA^T - OC^T V_2^{-1} C P + V_1 = 0 \tag{25}$$

Using the estimated states, the control force of the MR mount is obtained as follows.

$$u(t) = -(k_1 \hat{q}_1(t) + k_2 \hat{\dot{q}}_1(t) + k_3 \hat{q}_2(t) + k_4 \hat{\dot{q}}_2(t) + k_5 \hat{q}_3(t) + k_6 \hat{\dot{q}}_3(t)) \tag{26}$$

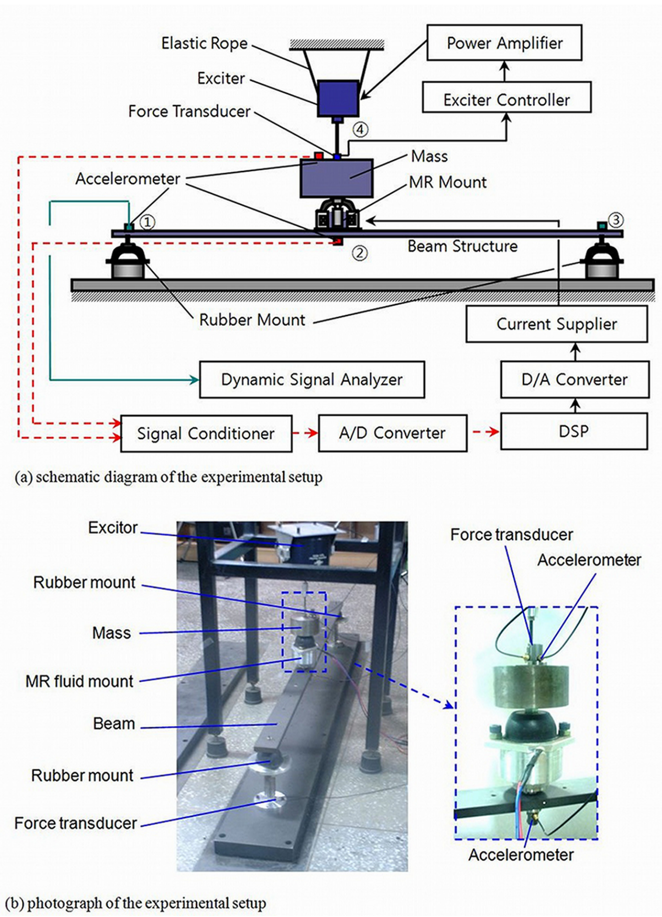

Figure 6. Experimental setup for vibration control.

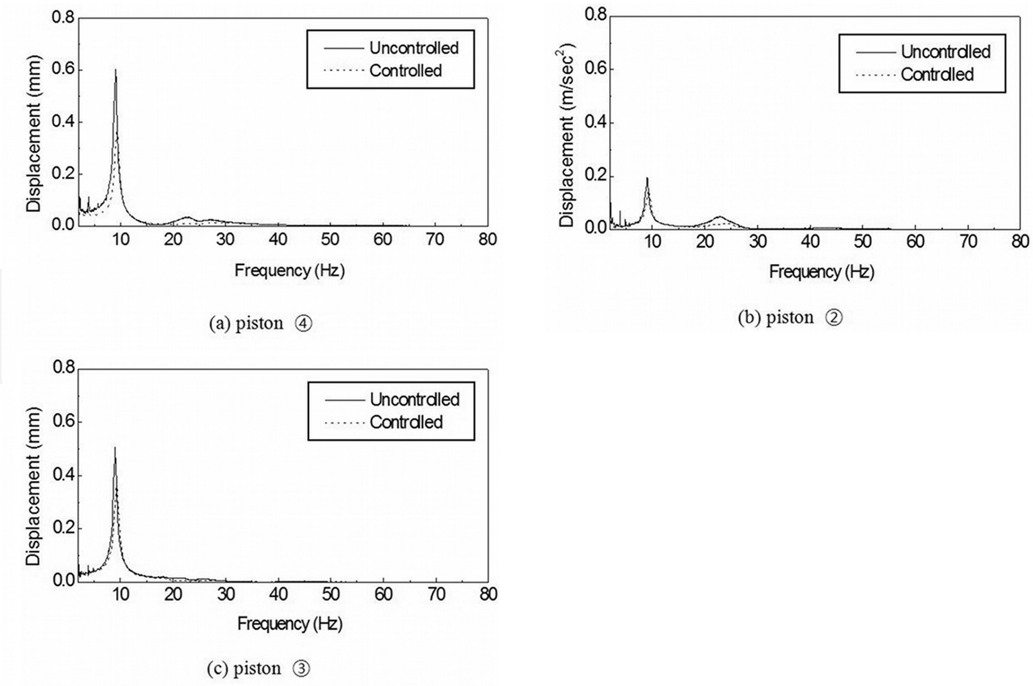

Figure 7. Displacement response of the structural system with the MR mount.

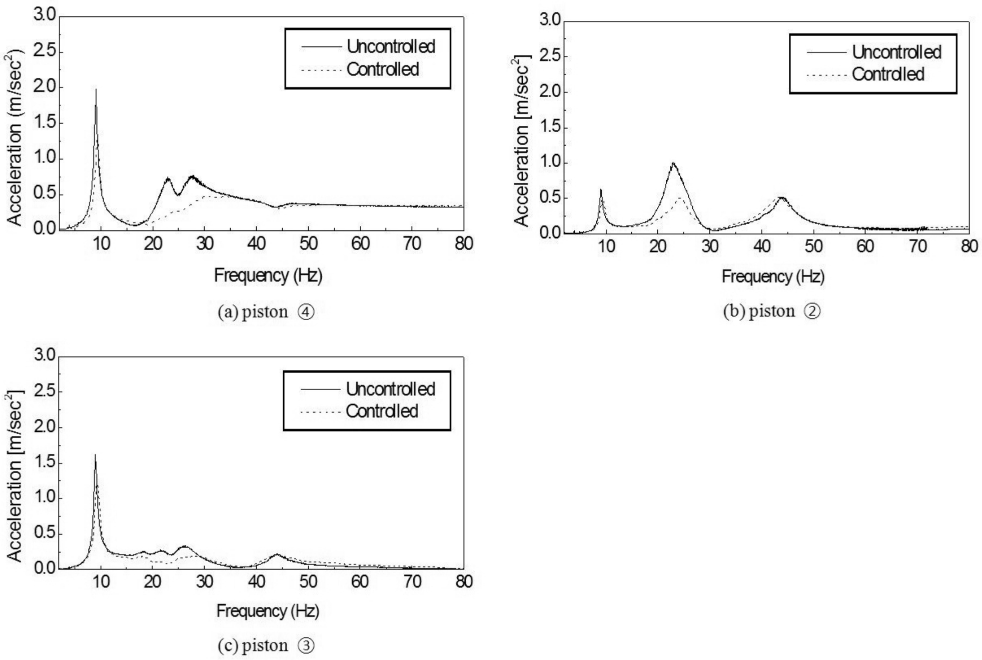

Figure 8. Acceleration response of the structural system with the MR mount.

In order to implement the LQG controller, an experimental setup is established as shown in Figure 6. The mass supported by the MR mount is excited by the electromagnetic exciter, and the excitation force and frequency are regulated by the exciter controller. Accelerometers are

http://dx.doi.org/10.5772/48823

attached to the beam and mass, and their positions are denoted by ▪ $(x = p_1)$, ▪ $(x = p_2)$, ▪ $(x = p_3)$, and ▪ $(x = p_4)$. Two accelerometers, attached on the positions ▪ and ▪, are used for the feedback signals. Velocity signals at these positions are obtained by using integrator circuit of charge amplifier. And the other accelerometers are used to measure vibration of the structural system. The velocity signal which denoted by dashed line in Figure 6 is fed back to the DSP (digital signal processor) via an A/D(analog to digital) converter. The state variables required for the LQR (26) are then estimated by the KBF (23), and control voltage is determined by means of the LQR controller in the DSP. The control current is applied to the MR mount via a D/A (digital to analog) converter and a current supplier. The sampling rate in the controller implementation is set by 2kHz.

Figures 7 and 8 present the measured displacement and acceleration of the structural system. The amplitude of excitations force is set by 1N. The excitation frequency range for the structural system is chosen from 5 to 80Hz. The uncontrolled and controlled responses are measured at the positions of the mass (▪) and beam structure (▪ , ▪). It is observed from Figures 7 and 8 that the resonant modes of the structural system have been reduced by controlling the damping force of the MR mount. Especially, the 2nd and 3rd modes vibration at the position ▪ has been substantially reduced by activating the MR mount. It is noted that the uncontrolled response is obtained without input current.

5. Conclusion

A new type of the mixed-mode MR mount was proposed and applied to vibration control of a flexible beam structure system. On the basis of non-dimensional Bingham number, an appropriate size of the MR mount was designed and manufactured. After experimentally evaluating the field-dependent damping force of the MR mount, a structural system consisting of a flexible beam and vibrating rigid mass was established. The governing equation of motion of the system was formulated and a linear quadratic Gaussian (LQG) controller was designed to attenuate the vibration of the structural system. It has been demonstrated through experimental realization that the imposed vibrations of the structural system such as acceleration and displacement are favorably reduced by activating the proposed MR mount associated with the optimal controller. The control results presented in this study are quite self-explanatory justifying that the proposed semi-active MR mount can be effectively utilized to the vibration control of various structural systems such as flexible robot arm and satellite appendages.

Acknowledgements

This work was partially supported by the National Research Foundation of Korea (NRF) grant funded by the Korea government (MEST)(No. 2010-0015090).

Author details

Seung-Bok Choi*, Sung Hoon Ha and Juncheol Jeon

*Address all correspondence to: seungbok@inha.ac.kr

Smart Structures and Systems Laboratory, Department of Mechanical Engineering, Inha University, Incheon 402-751,, Korea

References

[1] Crawley, E. F., & de Luis, J. (1987). Use of Piezoelectric Actuators as Elements of Intelligent Structures. *AIAA Journal*, 25(10), 1373-1385.

[2] Choi, S. B., & Kim, M. S. (1997). New Discrete-Time Fuzzy-Sliding Mode Control with Application to Smart Structures. *AIAA Journal of Guidance, Control and Dynamics*, 20(5), 857-864.

[3] Roger, C. A. (1990). Active Vibration and Structural Acoustic Control of Shape Memory Alloy Hybrid Composites: Experimental Results. *Journal of Acoustical Society of America*, 88(6), 2803-2811.

[4] Choi, S. B., & Cheong, C. C. (1996). Vibration Control of a Flexible Beam Using SMA Actuators. *AIAA Journal of Guidance, Control, and Dynamics*, 19(5), 1178-1180.

[5] Choi, S. B., Park, Y. K., & Jung, S. B. (1999). Modal Characteristics of a Flexible Smart Plate Filled with Electrorheological Fluids. *AIAA Journal of Aircraft*, 36(2), 458-464.

[6] Choi, S. B. (1999). Vibration Control of a Flexible Structure Using ER Dampers. *ASME Journal of Dynamic Systems, Measurement and Control*, 121(1), 134-138.

[7] Hong, S. R., & Choi, S. B. (2003). Vibration Control of a Structural System using Magneto-rheological Fluid Mount. *Proceedings of the 14th International Conference on Adaptive Structures and Technologies*, 182-194, (Seoul, Korea).

[8] Ushijima, T. K., Takano, K., & Kojima, H. (1988). High Performance Hydraulic Mount for Improving Vehicle Noise and Vibration. *SAE Technical Paper Series. 880073*.

[9] Tanaka, N., & Kikushima, Y. (1998). Optimal Design of Active Vibration Isolation Systems. *Transactions of the ASME, Journal of Vibration, Acoustics, Stress and Reliability in Design*, 110(1), 42-48.

[10] Hong, S. R., Choi, S. B., & Han, M. S. (2002). Vibration Control of a Frame Structure using Electrorheological Fluid Mounts. *International Journal of Mechanical Sciences*, 44(10), 2027-2045.

[11] Williams, E. W., Rigby, S. G., Sproston, J. L., & Stanway, R. (1993). Electrorheological Fluids Applied to an Automotive Engine Mount. *Journal of Non-Newtonian Fluid Mechanics*, 47, 221-238.

[12] Hong, S. R., Choi, S. B., Choi, Y. T., & Wereley, N. M. (2003). Comparison of Damping Force Models for an Electrorheological Fluid Damper. *International Journal of Vehicle Design*, 33(1-3), 17-35.

[13] Meirovitch, L. (1990). Dynamics and Control of Structures. John Wiley & Sons Inc.

[14] Machejowski, J. M. (1989). Multivariable feedback design. Addison-Wesley Publishing Company.

[15] Karnopp, D. (1990). Design Principles for Vibration Control Systems using Semi-active Dampers. *Journal of Dynamic Systems, Measurement and Control*, 112(3), 448-455.

IntechOpen

IntechOpen